The origin of the first sharp diffraction peak in liquid Na-Pb alloys: *ab initio* molecular-dynamics simulations

1999 J. Phys.: Condens. Matter 11 2199

(http://iopscience.iop.org/0953-8984/11/10/007)

J. Phys.: Condens. Matter **11** (1999) 2199–2210. Printed in the UK PII: S0953-8984(99)98907-5

The origin of the first sharp diffraction peak in liquid Na–Pb alloys: *ab initio* molecular-dynamics simulations

Y Senda, F Shimojo and K Hoshino

Faculty of Integrated Arts and Sciences, Hiroshima University, Higashi-Hiroshima 739-8521, Japan

Received 3 November 1998

Abstract. *Ab initio* molecular-dynamics simulations are carried out for liquid $Na_{0.8}Pb_{0.2}$ and $Na_{0.5}Pb_{0.5}$ alloys to investigate the ionic structure, the electronic states and especially the existence of the so-called 'Zintl ion' Pb_4^{4-} and the chemical complex Na_4Pb. In our simulation, the existence of these chemical units is not confirmed, but rather the intermediate-range ordering of Pb ions is seen in the liquid $Na_{0.8}Pb_{0.2}$ alloy. It is found from the calculated partial and total structure factors that this ordering of Pb ions leads to the first sharp diffraction peak of the total structure factor, which agrees well with the results of the neutron diffraction experiment. The composition dependence of the electronic states is explained on the basis of the ionic configuration. A tendency towards ionicity or charge transfer is seen in both liquid alloys, though the valence-electronic charge distribution is not so localized around the ions.

1. Introduction

Among the variety of liquid alloys, the liquid-alkali–Pb alloys are well known as compound-forming liquid alloys, in which structural properties, thermal properties and the electrical resistivity show characteristic behaviours near 'stoichiometric' compositions [1–5]. The primary observation is the shift of the position of the resistivity maximum from approximately 20% Pb to 50% Pb when going from Li–Pb to K–Pb [6]. The liquid Li–Pb alloy has been studied extensively, and the existence and the stability of the so-called 'octet compound' (Li_4Pb cluster) were suggested [7], while the existence of the Pb_4^{4-} tetrahedron, a so-called 'Zintl ion' [8] was assumed for the liquid K–Pb, Rb–Pb and Cs–Pb alloys. The liquid Na–Pb alloy studied in this paper has been considered to be a transition case between Li–Pb and K–Pb [9].

The crystalline compound NaPb includes tetrahedral Pb_4^{4-} clusters separated from each other by the Na atoms, which is the same structure as the NaSn compound has, while the compound $Na_{15}Pb_4$ which is close to the octet composition has such a structure that Pb atoms are surrounded only by the Na atoms. For the liquid Na–Pb alloy, the anomalously large electrical resistivity, the negative entropy of mixing and the first sharp diffraction peak (FSDP) of the structure factor were observed at the composition of $Na_{0.8}Pb_{0.2}$ [10, 11]. To explain these experimental results, a variety of models assuming the existence of a chemical complex in the liquid have been proposed. The structure factor of the liquid Na–Pb alloy was calculated using the formula for a three-component hard-sphere system [12], on the basis of the assumption that the liquid Na–Pb alloy is a mixture of Na, Pb and Na_4Pb [13, 14], as was assumed for the liquid Li–Pb alloy [7]. On the other hand, assuming the existence of Pb_4^{4-} tetrahedra in the liquid Na–Pb alloy as was done for liquid K–Pb, Rb–Pb and Cs–Pb systems, a classical molecular-dynamics simulation was carried out [8], in which the Pb atoms are arranged in

0953-8984/99/102199+12$19.50

regular tetrahedra, while the Na atoms were assumed to be monovalent, positively charged ions. These calculated structure factors appeared to agree fairly well with the observed ones, though the existence of the chemical complex Na_4Pb or the Pb_4^{4-} tetrahedron has not been directly confirmed yet.

An *ab initio* molecular-dynamics (MD) simulation is a very effective and successful tool for describing liquid alloys in which the correlation between the ionic configuration and the electronic states plays an important role [15]. Recently, *ab initio* MD simulation has been applied to several liquid alloys [16–18], and contributed to a better understanding of those liquid alloys. The *ab initio* MD simulation of the liquid $Cs_{0.5}Pb_{0.5}$ alloy was carried out by de Wijs *et al* [17] and it was shown that the remnants of the Pb_4^{4-} tetrahedra which exist in the solid state were found, though most of them were destroyed, and more complex structures were present. Quite recently, Seifert *et al* [18] applied *ab initio* MD simulation to the liquid Na–Sn alloys for five compositions. They showed that the Zintl ions Sn_4^{4-} could not be found and that Sn ions form a dynamic network structure in the liquid $Na_{0.5}Sn_{0.5}$ alloy. For the liquid $Na_{0.8}Sn_{0.2}$ alloy, only isolated Sn atoms or dimers exist, in contrast to the suggestion of the existence of the 'octet compound' Na_4Sn as in the case of liquid $Na_{0.8}Pb_{0.2}$ alloy.

In this paper we apply *ab initio* MD simulation to liquid $Na_{0.8}Pb_{0.2}$ and $Na_{0.5}Pb_{0.5}$ alloys. The purposes of this paper are (1) to investigate the composition dependence of the chemical short-range order and the electronic states, (2) to provide a microscopic interpretation for the observed characteristic features and (3) to clarify the origin of the first sharp diffraction peak.

In section 2 we briefly summarize the method of our *ab initio* MD simulation. In section 3, the results of our calculation are given and discussed in comparison with experiment. Finally, the conclusions are given in section 4.

2. Method

To study the structure and the electronic states of liquid Na–Pb alloys, we carry out an *ab initio* MD simulation, which is based on the density functional theory in the local-density approximation, the pseudopotential theory and the adiabatic approximation. We minimize the Kohn–Sham energy functional for a given ionic configuration by the conjugate-gradient method [19, 20] and calculate the electron density and the forces acting on ions based on the Hellmann–Feynman theorem. We use the norm-conserving pseudopotential proposed by Troullier and Martins [21] for both Na and Pb atoms. The Pb pseudopotential is generated from the scalar-relativistic atomic calculation [22]. The non-local part is calculated using the Kleinman–Bylander separable form [23]. The exchange–correlation energy is calculated in the local-density approximation [24, 25]. The partial-core correction [26] is taken into account in order to guarantee the transferability of the pseudopotentials employed. The fractional occupancies of energy levels are introduced in order to ensure the convergence of the electronic states of metals. The wavefunction, sampled at only the Γ point of the Brillouin zone, is expanded in plane waves and their cut-off energy is 10 Ryd, which is determined so as to converge the total energy to within 1 mRyd/electron.

In our calculations, we use a cubic supercell and the periodic boundary condition is imposed. The total number of atoms in the supercell is taken to be one hundred and the volume of the supercell is determined using the observed densities of the liquid alloys. The side of the cubic cell is about 15 Å. As an initial configuration, Na and Pb atoms are randomly arranged on the simple cubic lattice.

A constant-temperature MD simulation is carried out using the Nosé–Hoover thermostat technique [27, 28]. The classical equations of motion are solved using the velocity Verlet algorithm. Our simulation is carried out for 3.6 ps with the time step of 2.4 fs and at the

temperature of 700 K, which is above the liquidus temperatures 659 K for $Na_{0.8}Pb_{0.2}$ and 645 K for $Na_{0.5}Pb_{0.5}$.

3. Results and discussion

3.1. Structural properties

3.1.1. The ionic configuration. In figures 1(a) and 1(b) we show snapshots of ionic configurations obtained by our *ab initio* MD simulation for the liquid $Na_{0.8}Pb_{0.2}$ and $Na_{0.5}Pb_{0.5}$ alloys, respectively. For the liquid $Na_{0.8}Pb_{0.2}$ alloy, it is seen from figure 1(a) that the Pb ions

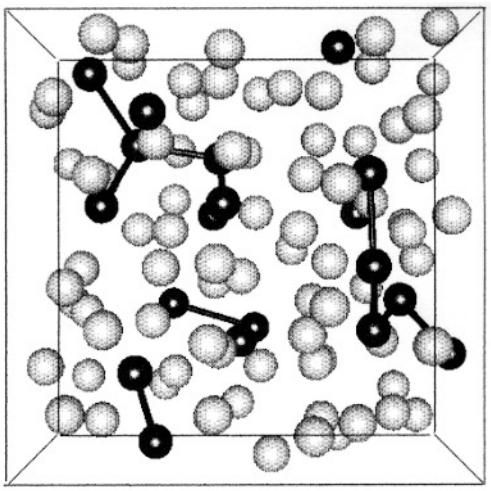

(a)

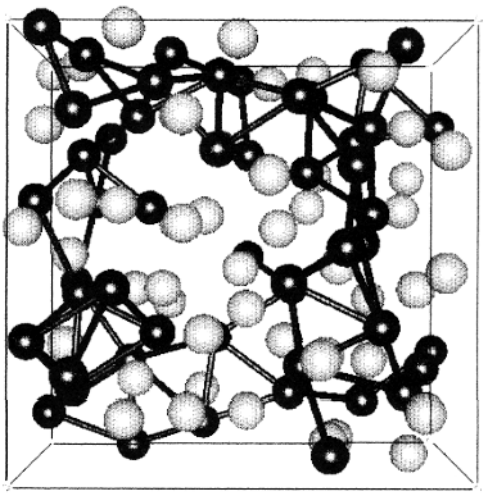

(b)

Figure 1. Snapshots of ionic configurations for the liquid (a) $Na_{0.8}Pb_{0.2}$ and (b) $Na_{0.5}Pb_{0.5}$ alloys. Pb and Na ions are shown as black and white balls, respectively. The Pb–Pb bonds are drawn for Pb-ion pairs within the cut-off distance of 4.0 Å.

displayed as black balls form small clusters, while some Pb ions exist as isolated ions. The bonds between Pb ions are drawn for Pb-ion pairs with separations less than 4 Å, which is the radius of the first coordination shell of $g_{\mathrm{PbPb}}(r)$ as will be shown in figure 3—see below. During the simulation, the tetrahedral Zintl ion Pb_4^{4-} did not survive as a stable cluster, i.e. the Pb tetrahedra broke down for a short time and turned into dimers or trimers. For the liquid $Na_{0.5}Pb_{0.5}$ alloy, a network of Pb ions is formed as is seen from figure 1(b) and no Zintl ion was observed as an *isolated* cluster as is seen for the crystalline NaPb compound within our simulation. It is interesting to note that the characteristic features of the ionic configurations obtained for the liquid $Na_{0.8}Pb_{0.2}$ and $Na_{0.5}Pb_{0.5}$ alloys are very similar to those obtained for the liquid Na–Sn alloys [18], except for the occurrence of the stable dimers Sn_2 in the liquid $Na_{0.8}Sn_{0.2}$ alloys.

We show the trajectory-averaged Pb–Pb–Pb and Na–Pb–Na bond-angle distributions in figure 2. As is seen in the Pb–Pb–Pb bond-angle distribution, there is only a low small peak at 60° for the liquid $Na_{0.8}Pb_{0.2}$ alloy, which is consistent with the absence of the Pb_4^{4-}, and there is a high peak at 60° for the liquid $Na_{0.5}Pb_{0.5}$ alloy, which corresponds to the fact that there exist many fragments of Pb_4^{4-} in the network structure as is seen in figure 1(b). From the Na–Pb–Na bond-angle distribution, we cannot find any indication for the existence of the compound Na_4Pb, since there is no peak at 109°.

In figure 3 we show the partial radial distribution functions $g_{\mathrm{NaNa}}(r)$, $g_{\mathrm{NaPb}}(r)$ and $g_{\mathrm{PbPb}}(r)$ calculated for the liquid $Na_{0.8}Pb_{0.2}$ and $Na_{0.5}Pb_{0.5}$ alloys. The average coordination numbers, i.e. the average numbers of ions of the jth species around an ion of the ith species, are estimated

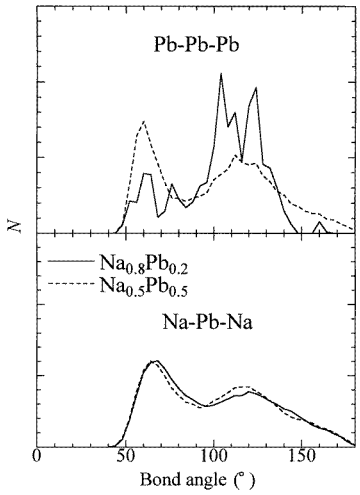

Figure 2. The bond-angle distributions for the liquid $Na_{0.8}Pb_{0.2}$ (full curve) and $Na_{0.5}Pb_{0.5}$ (broken curve) alloys.

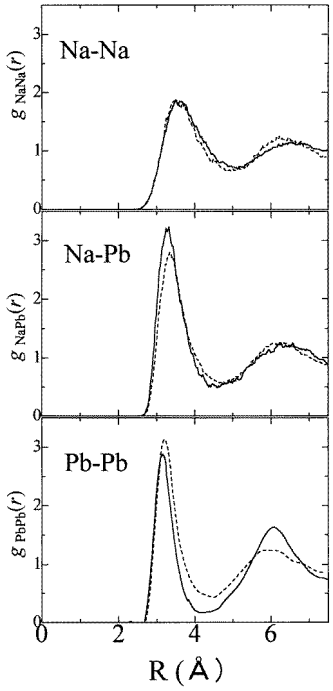

Figure 3. The partial radial distribution functions for the liquid $Na_{0.8}Pb_{0.2}$ (full curve) and $Na_{0.5}Pb_{0.5}$ (broken curve) alloys.

Table 1. The average coordination numbers.

	$Na_{0.8}Pb_{0.2}$	$Na_{0.5}Pb_{0.5}$
Na atoms around an Pb atom	5.0	3.6
Pb atoms around an Pb atom	1.2	4.5
Na atoms around a Na atom	5.2	3.7

from the formula

$$2\rho_j \int_0^{r_{ij}} 4\pi r^2 g_{ij}(r)\,\mathrm{d}r$$

where ρ_j is the number density of atoms of the jth species and r_{ij} the first-peak position of the $g_{ij}(r)$. The average coordination numbers thus estimated are shown in table 1. It should be noted for the liquid $Na_{0.8}Pb_{0.2}$ alloy that the first minimum and the second peak of the $g_{\mathrm{PbPb}}(r)$ are relatively deeper and higher, respectively, as compared with typical partial radial distribution functions for ordinary liquid binary alloys. $g_{\mathrm{PbPb}}(r)$ for the liquid $Na_{0.5}Pb_{0.5}$ alloy has a standard form.

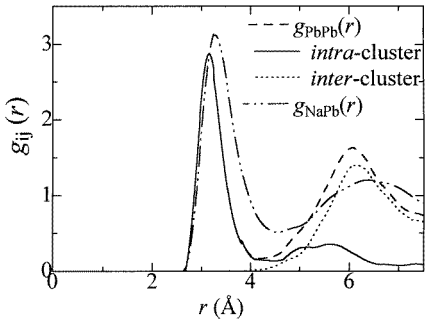

Figure 4. The contributions to $g_{\mathrm{PbPb}}(r)$ (broken curve) for the liquid $Na_{0.8}Pb_{0.2}$ alloy from the intra-cluster correlation of Pb ions (solid curve) and from the inter-cluster correlation of Pb ions (dotted curve). $g_{\mathrm{PbNa}}(r)$ is also shown by a dashed–double-dotted curve.

To explain the characteristic features of $g_{\mathrm{PbPb}}(r)$ for the liquid $Na_{0.8}Pb_{0.2}$ alloy shown in figure 3, we show in figure 4 the two contributions to $g_{\mathrm{PbPb}}(r)$ from the correlation of Pb ions within the cluster (*intra*-cluster) and from that between the clusters (*inter*-cluster). Here, we define a cluster as the unit of Pb atoms which are connected with bonds as shown in figure 1. $g_{\mathrm{NaPb}}(r)$ is also shown in figure 4. It can be seen from figure 4 that the first peak of $g_{\mathrm{PbPb}}(r)$ is dominated by the intra-cluster correlation of Pb ions, while the high second peak at around $r = 6$ Å comes from the inter-cluster correlation of Pb ions. The average coordination number of Pb ions around a Pb ion is about one, which means that there are not so many Pb clusters and the clusters are very small ones, as is seen from figure 1(a). It is also seen from $g_{\mathrm{NaPb}}(r)$ shown in figure 4 that a considerable number of Na ions are located in the region of the first minimum of $g_{\mathrm{PbPb}}(r)$, which is consistent with the fact that there are small Pb clusters separated by the Na ions, as shown in figure 1(a). Such an intermediate-range ordering of Pb ions reflects on the characteristic features of $g_{\mathrm{PbPb}}(r)$ for the liquid $Na_{0.8}Pb_{0.2}$ alloy.

3.1.2. The structure factor. To discuss the short- or intermediate-range ordering of Na and Pb ions, it is useful to investigate the concentration–concentration structure factor $S_{CC}(k)$, which

is defined by

$$S_{CC}(k) = c_{\mathrm{Na}}c_{\mathrm{Pb}}[c_{\mathrm{Pb}}S_{\mathrm{NaNa}}(k) + c_{\mathrm{Na}}S_{\mathrm{PbPb}}(k) - 2(c_{\mathrm{Na}}c_{\mathrm{Pb}})^{1/2}S_{\mathrm{NaPb}}(k)] \tag{1}$$

where c_i is the concentration of the ith species and $S_{\mathrm{NaNa}}(k)$, $S_{\mathrm{PbPb}}(k)$ and $S_{\mathrm{NaPb}}(k)$ are partial structure factors in the Ashcroft–Langreth (AL) form. We have calculated the AL partial structure factors $S_{ij}(k)$ defined by

$$S_{ij}(k) = \frac{1}{(N_i N_{\mathrm{j}})^{1/2}}\left\langle \sum_{\mu=1}^{N_i}\sum_{\nu=1}^{N_{\mathrm{j}}} \mathrm{e}^{\mathrm{i}\boldsymbol{k}\cdot(\boldsymbol{r}_\mu - \boldsymbol{r}_\nu)} \right\rangle \tag{2}$$

using the positions of ions $\{\boldsymbol{r}_\mu\}$ obtained by our *ab initio* MD simulation. Here N_i is the number of ions of the ith species and the brackets $\langle\cdots\rangle$ mean the time average.

Figure 5 shows the AL partial structure factors calculated for the liquid $Na_{0.8}Pb_{0.2}$ and $Na_{0.5}Pb_{0.5}$ alloys. There is a prepeak on the low-k side of the main peak of $S_{\mathrm{PbPb}}(k)$ for the liquid $Na_{0.8}Pb_{0.2}$ alloy. The position of the prepeak is at $k \simeq 1.2$ Å^{-1}, which corresponds, using the rule of thumb $kr = 7.7$ [9], to the distance $r \simeq 6.0$ Å. This distance coincides with the position of the second peak of $g_{\mathrm{PbPb}}(r)$, which means that the intermediate-range ordering of Pb ions gives rise to the prepeak of the $S_{\mathrm{PbPb}}(k)$. On the other hand, for the liquid $Na_{0.5}Pb_{0.5}$ alloy, such an intermediate-range correlation of Pb ions is not clearly seen in $S_{\mathrm{PbPb}}(k)$ as well as in $g_{\mathrm{PbPb}}(r)$.

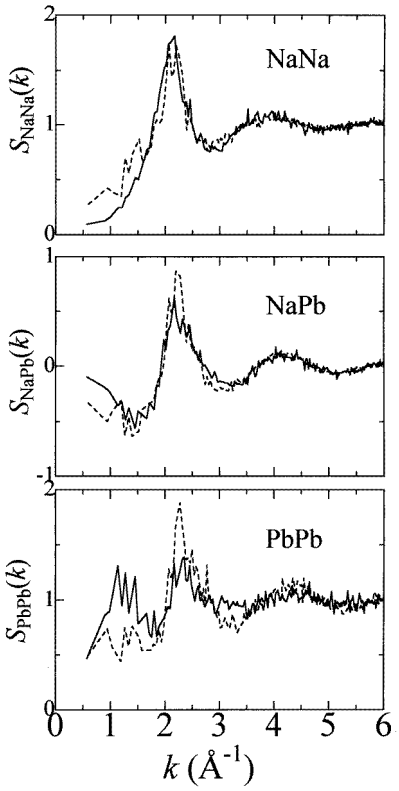

Figure 5. The Ashcroft–Langreth partial structure factors for the liquid $Na_{0.8}Pb_{0.2}$ (full curve) and $Na_{0.5}Pb_{0.5}$ (broken curve) alloys.

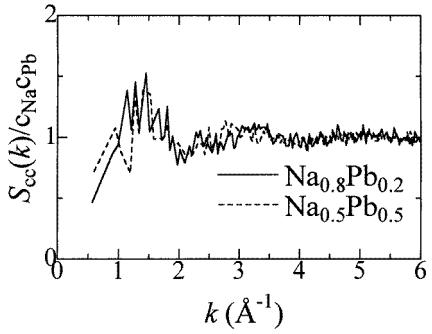

Figure 6. The concentration–concentration structure factors for the liquid $Na_{0.8}Pb_{0.2}$ (full curve) and $Na_{0.5}Pb_{0.5}$ (broken curve) alloys.

The $S_{CC}(k)$ for the liquid $Na_{0.8}Pb_{0.2}$ and $Na_{0.5}Pb_{0.5}$ alloys are shown in figure 6. There is a peak at $k \simeq 1.2$ Å^{-1}, which is due to the prepeak of $S_{PbPb}(k)$ for the liquid $Na_{0.8}Pb_{0.2}$ alloy shown in figure 5. The concentration–concentration correlation indicated by this peak is closely associated with the characteristic feature of the ionic configuration; the Pb clusters are separated by the Na ions as was mentioned before.

The total structure factor observed by means of the neutron diffraction is expressed as a linear combination of the AL partial structure factors $S_{ij}(k)$:

$$S(k) = \frac{c_{Na}b_{Na}^2 S_{NaNa}(k) + 2\sqrt{c_{Na}c_{Pb}}b_{Na}b_{Pb}S_{NaPb}(k) + c_{Pb}b_{Pb}^2 S_{PbPb}(k)}{c_{Na}b_{Na}^2 + c_{Pb}b_{Pb}^2} \tag{3}$$

where b_i is the neutron scattering length of the ith species; $b_{Na} = 0.363 \times 10^{-12}$ cm and $b_{Pb} = 0.940 \times 10^{-12}$ cm. The $S(k)$ thus obtained for the liquid $Na_{0.8}Pb_{0.2}$ and $Na_{0.5}Pb_{0.5}$ alloys are compared with the experimental results obtained by the neutron diffraction [11] in figure 7. Our results are in very good agreement with the observed $S(k)$ and the composition dependence of the FSDP of the $S(k)$ is especially well reproduced, i.e. the height of the FSDP is highest for the liquid $Na_{0.8}Pb_{0.2}$ alloy. It is obvious from equation (3) and from the partial structure factors $S_{ij}(k)$ shown in figure 5 that the most dominant contribution to the FSDP is due to the prepeak of the partial structure factor $S_{PbPb}(k)$. As was mentioned previously, this prepeak comes from the intermediate-range ordering of the Pb ions; therefore we can conclude that the FSDP is a result of such an ordering of the Pb ions. The height of the observed FSDP becomes lower for the liquid $Na_{0.5}Pb_{0.5}$ alloy, which is consistent with our result that the intermediate-range correlation of Pb ions is not clearly seen for the liquid $Na_{0.5}Pb_{0.5}$ alloy.

The broad peak at around $k = 4.0$ Å^{-1} of $S(k)$ for the liquid $Na_{0.8}Pb_{0.2}$ alloy shown in figure 7 comes from the difference in the second-peak positions of $S_{NaNa}(k)$ and $S_{PbPb}(k)$ shown in figure 5. This peak, on the other hand, becomes the ordinary one for the liquid $Na_{0.5}Pb_{0.5}$ alloy, since the contribution of $S_{NaNa}(k)$ to $S(k)$ decreases with decreasing Na concentration and only the second peak of $S_{PbPb}(k)$ is emphasized in $S(k)$ for the liquid

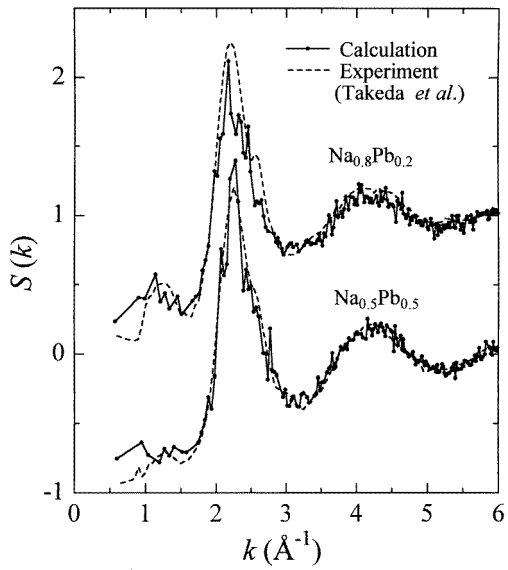

Figure 7. The total structure factors for the liquid $Na_{0.8}Pb_{0.2}$ and $Na_{0.5}Pb_{0.5}$ alloys compared with the results of the neutron scattering experiment [11].

$Na_{0.5}Pb_{0.5}$ alloy; the ratios of the coefficients for $S_{NaNa}(k)$ and $S_{PbPb}(k)$ in equation (3) are as follows: $c_{Na}b_{Na}^2/c_{Pb}b_{Pb}^2 = 0.60$ for $Na_{0.8}Pb_{0.2}$ and 0.15 for $Na_{0.5}Pb_{0.5}$ alloy, and therefore the contribution of $S_{NaNa}(k)$ to $S(k)$ is relatively small in the latter.

3.2. Electronic properties

3.2.1. The electronic density of states. We show in figures 8 and 9 the total and the partial electronic densities of states (DOS), respectively, which are obtained by sampling ten k-points of the Brillouin zone and by averaging over some ionic configurations. The lth component of the partial DOS of the ith species is calculated by projecting the wavefunctions on the spherical harmonics within a sphere of radius R_c centred at each μth atom of the ith species, the position of which is $\boldsymbol{r}_\mu$ as follows:

$$D_i^l(\epsilon) = \sum_{\mu=1}^{N_i}\sum_{\alpha}\sum_{m=-l}^{l}\int_0^{R_c}|\boldsymbol{r}-\boldsymbol{r}_\mu|^2\,\mathrm{d}|\boldsymbol{r}-\boldsymbol{r}_\mu|\left|\int Y_{lm}^*(\Omega_\mu)\psi_\alpha(\boldsymbol{r})\,\mathrm{d}\Omega_\mu\right|^2\delta(\epsilon-\epsilon_\alpha)\Big/N_i \tag{4}$$

where N_i is the number of ions of the ith species, ψ_α is the wavefunction of the αth state which has the eigenvalue ϵ_α and the $Y_{lm}(\Omega_\mu)$ are spherical harmonics with an angular momentum l, which is centred at the μth ion. R_c is chosen to be about the half of the average nearest-

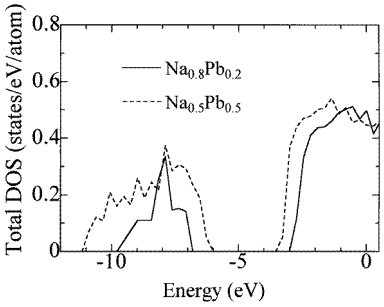

Figure 8. The total densities of states for the liquid $Na_{0.8}Pb_{0.2}$ and $Na_{0.5}Pb_{0.5}$ alloys.

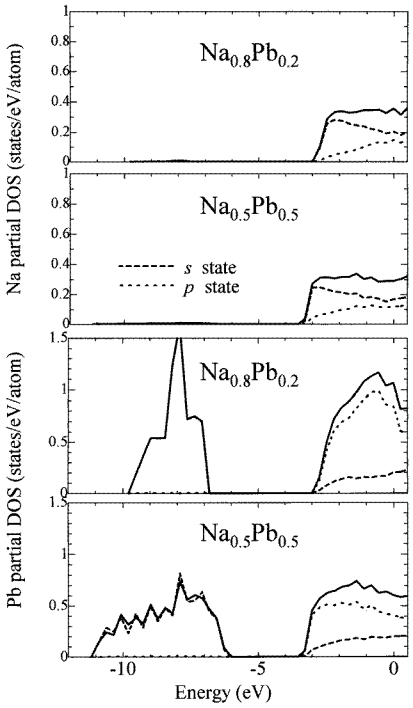

Figure 9. The partial densities of states for the liquid $Na_{0.8}Pb_{0.2}$ and $Na_{0.5}Pb_{0.5}$ alloys. The decompositions of the partial DOSs into s (broken curve) and p (dotted curve) components are shown for Na in the upper two panels and for Pb in the lower two panels.

neighbour distance, on which the partial DOS does not depend significantly. The origin of the energy is taken to be the Fermi level.

The electronic states at around −8 eV come from the Pb 6s states and those above −3 eV come from the hybridization of the Pb 6p and the Na 3s states. As is seen from figure 8, the bands become broader as the concentration of Pb atoms increases. The partial DOS of Pb decreases rapidly around the Fermi level for the liquid $Na_{0.8}Pb_{0.2}$ alloy, though the total DOS around the Fermi level does not depend so much on the composition.

The electronic states are closely related to the ionic configuration. As is seen from figure 1, there are small clusters of Pb ions as well as isolated Pb ions in the liquid $Na_{0.8}Pb_{0.2}$ alloy, though there exists a large network of Pb ions in the liquid $Na_{0.5}Pb_{0.5}$ alloy. Therefore the overlap of the wavefunctions of Pb is smaller in the former than in the latter and, as a result, gives rise to narrower energy bands in the former. This tendency is more evident for the lower band because it mainly comes from the Pb 6s states. In the upper band dominated by the hybridization of the Pb 6p and the Na 3s states, the centre of mass of the energy band shifts to the lower energy as the Pb concentration increases, since the energy level of the Pb 6p state is lower than that of the Na 3s state.

The DOSs obtained by our *ab initio* MD simulation for the liquid $Na_{0.8}Pb_{0.2}$ and $Na_{0.5}Pb_{0.5}$ alloys are similar to those for the crystalline compounds $Na_{15}Pb_4$ and NaPb, respectively, which were calculated by Tegze and Hafner [29] using the linear muffin-tin orbital method. They showed that the electronic structure is dominated by the strong attractive Pb potential at all compositions and that the bandwidth becomes broader as the volume per Pb atom decreases. The observed excess volume per atom is negative with a strongest relative deviation at the composition close to that of the liquid $Na_{0.5}Pb_{0.5}$ alloy, in which the volume per Pb atom can be estimated to be smaller than that of the liquid $Na_{0.8}Pb_{0.2}$ alloy. The characteristic feature seen for the crystalline-alkali–Pb compound is found also for the liquid alloys.

3.2.2. Charge transfer. Because of the large difference in electronegativity between Na and Pb atoms (the electronegativity on Pauling's scale is 0.93 for Na atoms and 2.33 for Pb atoms), their mixture has been expected to have an ionic character, i.e. to show some amounts of electronic charge transfer from the Na atom to the Pb atom. Experimentally, physical properties show anomalous behaviour at the 'stoichiometric' composition of $Na_{0.8}Pb_{0.2}$, which has been considered to be the most favourable composition for the ionicity from the point of view of complete electron transfer and construction of the closed shell of the Pb atom. The classical MD simulation for this liquid alloy [8], as was mentioned in the introduction, was carried out using the ionic model, assuming that one electron is transferred from a Na atom to Pb atoms.

From our study we found that the liquid $Na_{0.8}Pb_{0.2}$ alloy is not as ionic as was expected; e.g. the charge transfer from Na to Pb atoms is not so large as is seen from the occupied partial DOS of the Na atom shown in figure 9. The electron-density distribution obtained by the present calculations indicates that considerable numbers of valence electrons remain around Na ions. However, these do not indicate the absence of ionicity. We investigate the ionicity of the liquid as follows: figures 10(a) and 10(b) show the 'difference' of the electron-density distribution $\rho(\boldsymbol{r})$ for the ionic configuration shown from the sum of the atomic electron-density distributions $\rho_{\mathrm{atom}}(\boldsymbol{r})$ for liquid $Na_{0.8}Pb_{0.2}$ and $Na_{0.5}Pb_{0.5}$ alloys, respectively, calculated from

$$\Delta\rho(\boldsymbol{r}) = \rho(\boldsymbol{r}) - \sum_{\mu} \rho_{\mathrm{atom}}(|\boldsymbol{r} - \boldsymbol{r}_{\mu}|) \tag{5}$$

where the $\boldsymbol{r}_{\mu}$ is the position of the μth atom of the corresponding ionic configuration shown in figures 10(a) and 10(b). The blue region has $\Delta\rho(\boldsymbol{r}) < 0$ and the red one has $\Delta\rho(\boldsymbol{r}) > 0$. When the ions are on the plane where the electron-density distribution is calculated, the core

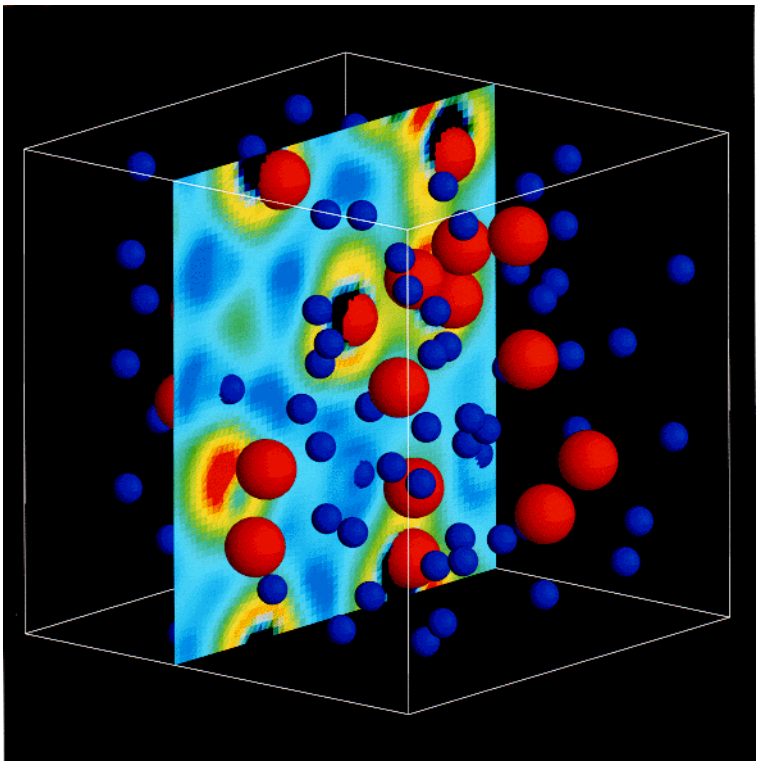

(a)

Figure 10. The electron-density distributions for the ionic configurations of the liquid (a) $Na_{0.8}Pb_{0.2}$ and (b) $Na_{0.5}Pb_{0.5}$ alloys. The Na and Pb ions are shown as blue and red balls, respectively.

regions are shown by black holes, since $\Delta\rho(\boldsymbol{r}) < 0$ and $|\Delta\rho(\boldsymbol{r})| \ll \rho_0$ in those regions, ρ_0 being the average electron density.

It is seen that the regions around Na ions are dominated by blue regions, while those around Pb ions are dominated by red regions. This means that the charge transfer occurs from Na atoms to Pb atoms. It is seen from figures 10(a) and 10(b) that the charge transfer occurs in both liquid $Na_{0.8}Pb_{0.2}$ and $Na_{0.5}Pb_{0.5}$ alloys. The quantitative estimation of the electronic charge transfer, however, cannot be well defined, since the electronic charge is not so localized around the ions and rather spreads spatially. It may be said at least that the Na atoms 'partially' transfer their valence electrons to the Pb atoms.

This ionicity leads to some kind of charge ordering. The prepeak in $S_{CC}(k)$ in figure 6 indicates that the positively charged Na cations are located between the negatively charged Pb clusters, though this ordering is, of course, different from that of a typical ionic liquid such as molten salt, Na^+Cl^-.

4. Conclusions

We have carried out an *ab initio* molecular-dynamics simulation for the liquid $Na_{0.8}Pb_{0.2}$ and $Na_{0.5}Pb_{0.5}$ alloys to investigate the ionic structure, the electronic states and especially the existence of the Zintl ion Pb_4^{4-} or the compound Na_4Pb. It is shown that these chemical units are not clearly seen as isolated chemical units, but rather the intermediate-range ordering of

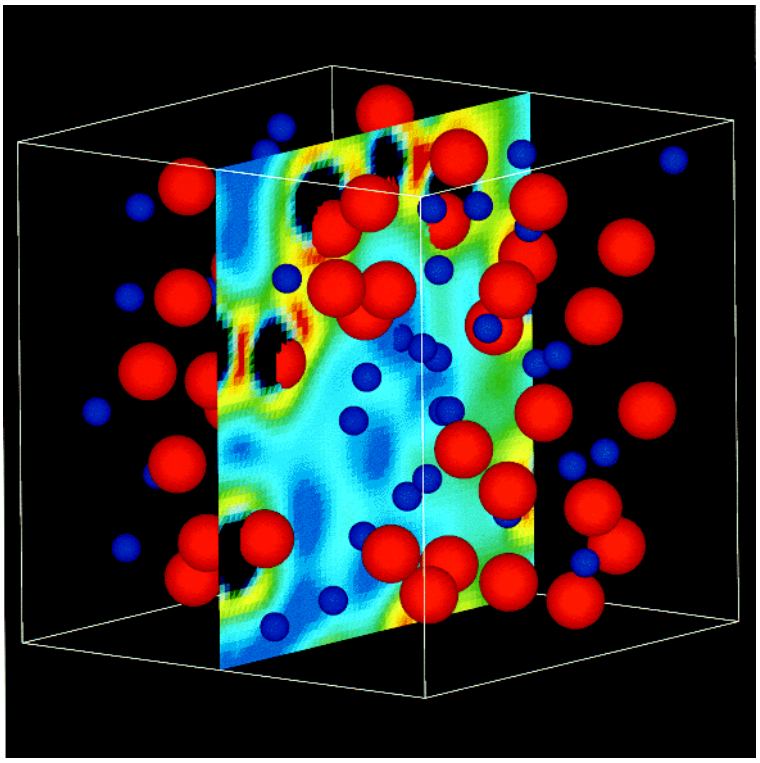

(b)

Figure 10. (Continued)

Pb ions is seen in the liquid $Na_{0.8}Pb_{0.2}$ alloy. It is found from the detailed analysis of the partial structure factors that this ordering of Pb ions comes from the correlation between the small clusters. Our calculations can quantitatively reproduce the total structure factors $S(k)$ observed by the neutron diffraction experiment and especially the composition dependence of the FSDP of $S(k)$. We found that the intermediate-range ordering of Pb ions leads to the FSDP of the total structure factor. The composition dependence of the electronic states is explained on the basis of the ionic configuration. The tendency towards becoming an ionic liquid is seen in both liquid alloys, though the valence-electronic charge distribution is not so localized around the ions.

Acknowledgments

We are grateful to Professor S Takeda for providing us with experimental data. We acknowledge Miss C Kitagawa and Mr H Asakura of KGT Incorporated for allowing us to use the visualization software AVS/Express Viz. This work was supported by Grant-in-Aids for Scientific Research (No 07236102, No 08304026 and No 10640370) from the Ministry of Education, Science, Sports and Culture, Japan. We thank the Computer Centre of the Institute for Molecular Science for allowing us to use the NEC SX-3/34R supercomputer. We also acknowledge the Centre for Promotion of Computational Science and Engineering (CCSE) of Japan Atomic Energy Research Institute (JAERI) for allowing us to use the NEC SX-4 and FUJITSU VPP300 supercomputers.

References

[1] Tumidajski P J, Petric A, Takenaka T, Pelton A D and Saboungi M-L 1990 *J. Phys.: Condens. Matter* **2** 209
[2] Saboungi M-L, Leonard S R and Ellefson J 1986 *J. Chem. Phys.* **85** 6072
[3] Saar J and Ruppersberg H 1988 *Z. Phys. Chem., NF* **156** 587
[4] Tumidajski P J 1991 *Can. Metall. Q.* **30** 271
[5] van der Marel C, Stein P C and van der Lugt W 1983 *Phys. Lett.* A **95** 451
[6] Meijer J A, Geertsma W and van der Lugt W 1985 *J. Phys. F: Met. Phys.* **15** 899
[7] Hoshino K and Young W H 1980 *J. Phys. F: Met. Phys.* **10** 1365
[8] Reijers H T A, van der Lugt W and Saboungi M-L 1990 *Phys. Rev.* B **42** 3395
[9] van der Lugt W 1996 *J. Phys.: Condens. Matter* **8** 6115
[10] van der Marel C, Oosten A B, Geertsma W and van der Lugt W 1982 *J. Phys. F: Met. Phys.* **12** 2349
[11] Takeda S, Harada S, Tamaki S, Matsubara E and Waseda Y 1987 *J. Phys. Soc. Japan* **56** 3934
[12] Hoshino K 1983 *J. Phys. F: Met. Phys.* **13** 1981
[13] Matsunaga S and Tamaki S 1983 *J. Phys. Soc. Japan* **52** 1725
[14] Takeda S, Tamaki S and Young W H 1990 *Phys. Chem. Liq.* **22** 51
[15] Senda Y, Shimojo F and Hoshino K 1998 *J. Phys. Soc. Japan* **67** 916
[16] Senda Y, Shimojo F and Hoshino K 1998 *J. Phys. Soc. Japan* **67** 2753
[17] de Wijs G A, Pastore G, Selloni A and van der Lugt W 1995 *J. Chem. Phys.* **103** 5031
[18] Seifert G, Kaschner R, Schöne M and Pastore G 1998 *J. Phys.: Condens. Matter* **10** 1175
[19] Kresse G and Hafner J 1994 *Phys. Rev.* B **49** 14 251
[20] Shimojo F, Zempo Y, Hoshino K and Watabe M 1995 *Phys. Rev.* B **52** 9320
[21] Troullier N and Martins J L 1991 *Phys. Rev.* B **43** 1993
[22] Wood J H and Boring A M 1978 *Phys. Rev.* B **18** 2701
[23] Kleinman L and Bylander D M 1982 *Phys. Rev. Lett.* **48** 1425
[24] Ceperley D M and Alder B J 1980 *Phys. Rev. Lett.* **45** 566
[25] Perdew J P and Zunger A 1981 *Phys. Rev.* B **23** 5048
[26] Louie S G, Froyen S and Cohen M L 1982 *Phys. Rev.* B **26** 1738
[27] Nosé S 1984 *Mol. Phys.* **52** 255
[28] Hoover W G 1985 *Phys. Rev.* A **31** 1695
[29] Tegze M and Hafner J 1989 *Phys. Rev.* B **39** 8263